Supporting Information

Effects of Pt loading on the activity of Pt/γ-Ga_2O_3 for propane dehydrogenation

Salman Khan[a], Kaijie Wang[a], Zhaoshuo Ge[a], Lixia Bao[b], Yi Dai[a], Qi Liu[c], Daxin Shi[a]*, Qin Wu[a], Kangcheng Chen[a], Guiyuan Jiang[c], Hansheng Li[a], Yaoyuan Zhang[a]*

[a] Beijing Key Laboratory for Chemical Power Source and Green Catalysis, School of Chemistry and Chemical Engineering, Beijing Institute of Technology, Beijing, 100081, China

[b] Analysis and Testing Center, Beijing Institute of Technology, Beijing 102488, China

[c] State Key Laboratory of Heavy Oil Processing, China University of Petroleum Beijing, Beijing, 102249, China

*Correspondence to: shidaxin@bit.edu.cn; yaoyuan.zhang@bit.edu.cn

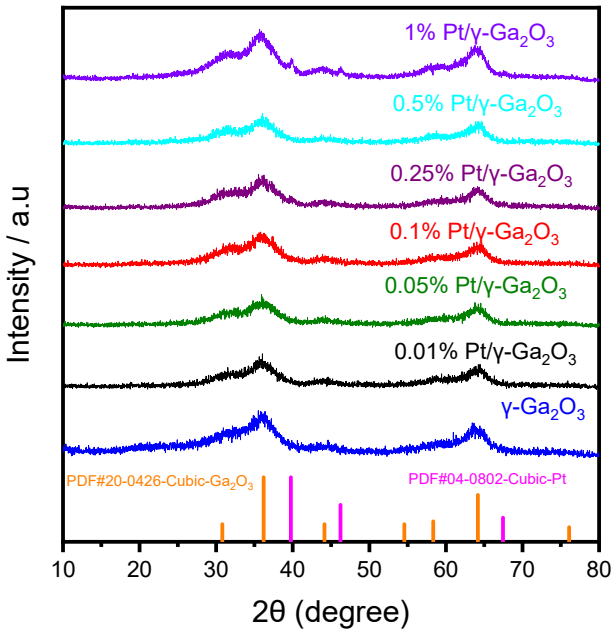

Figure S1 X-ray diffraction (XRD) patterns of different Ga_2O_3 catalyst prepared by different methods.

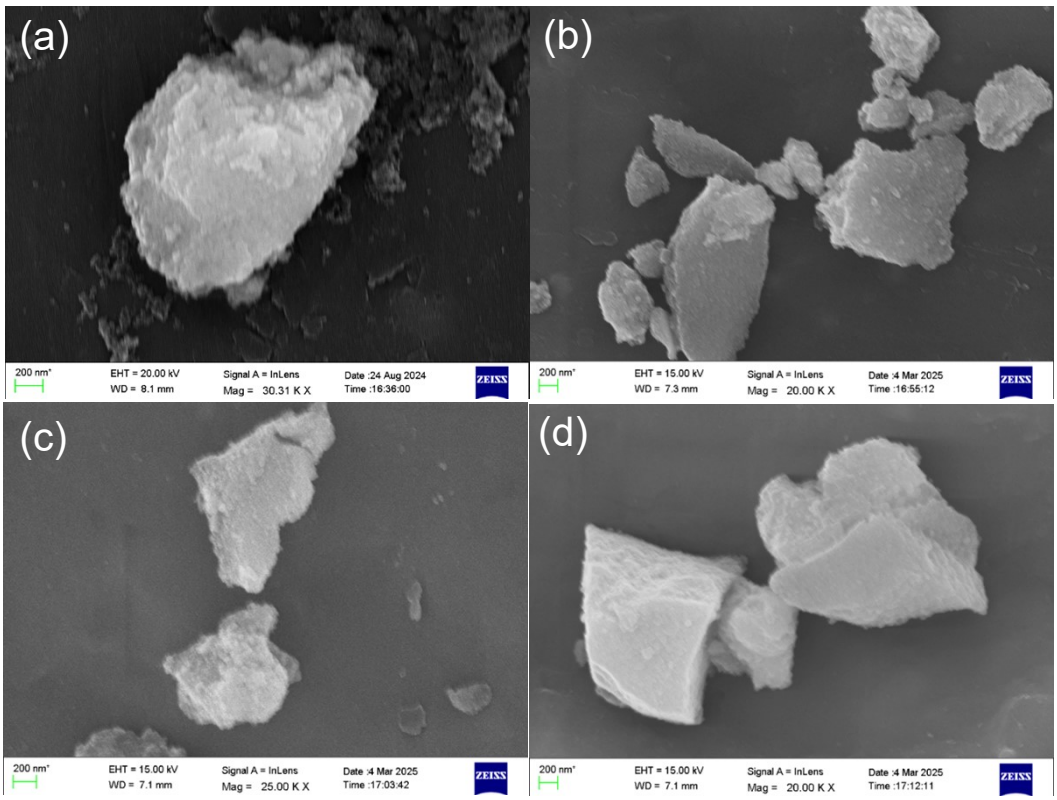

Figure S2 Scanning electron microscopy (SEM) images of (a) γ-Ga_2O_3, (b) 0.05% Pt/γ-Ga_2O_3, (c) 0.5% Pt/γ-Ga_2O_3, and (d) 1% Pt/γ-Ga_2O_3.

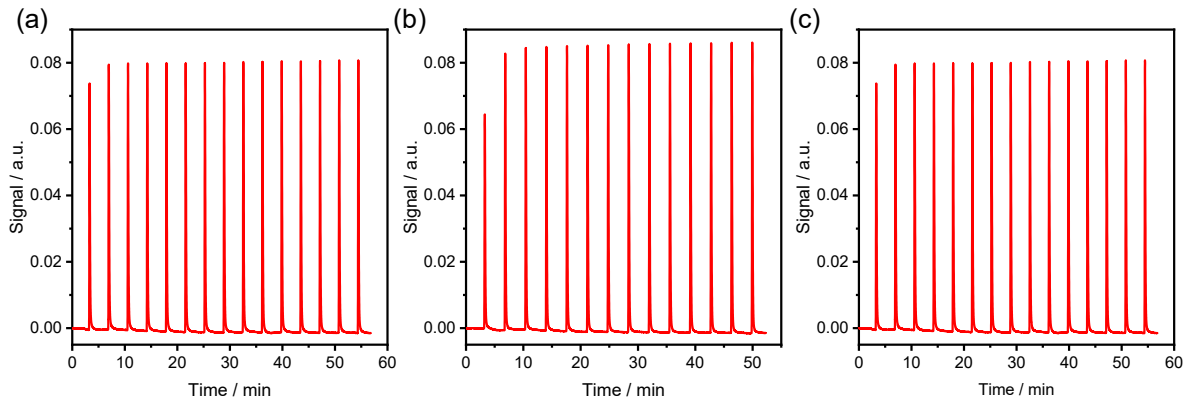

Figure S3 CO-pulse measurement of (a) 0.05% Pt/γ-Ga_2O_3, (b) 0.5% Pt/γ-Ga_2O_3, and (c) 1% Pt/γ-Ga_2O_3.

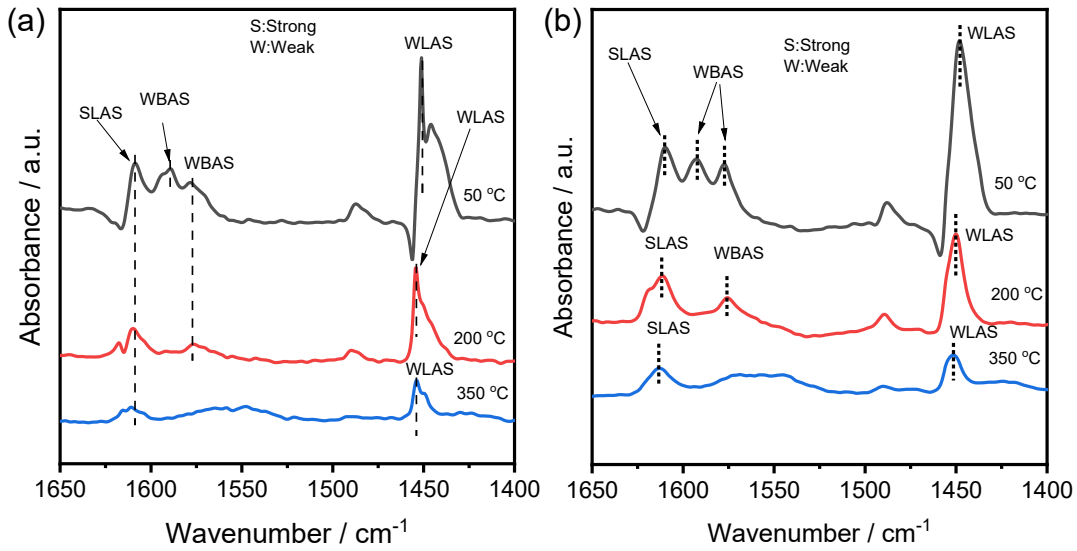

Figure S4 Pyridine-IR profiles obtained for (a) γ-Ga_2O_3 and (b) 1% Pt/γ-Ga_2O_3.

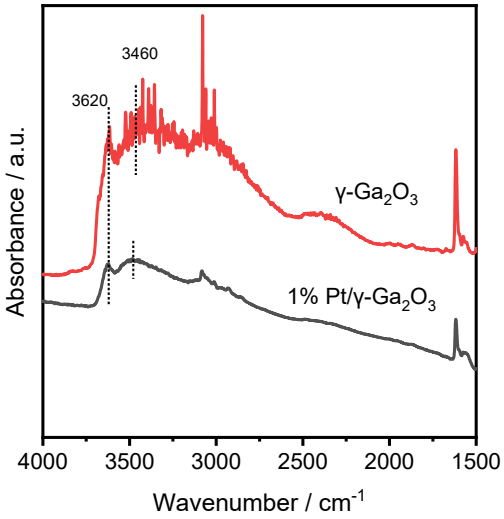

Figure S5 Fourier transform infrared spectroscopy (FTIR) spectra obtained for γ-Ga_2O_3 and 1% Pt/γ-Ga_2O_3.

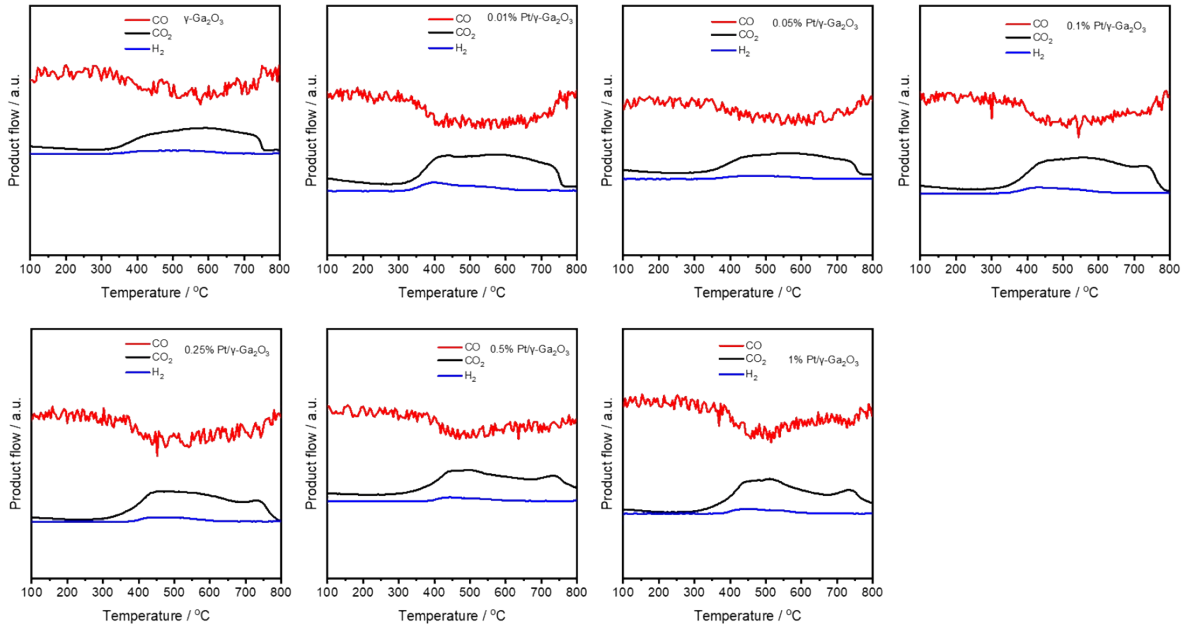

Figure S6 CO temperature-programmed reduction (CO-TPR) tests of different x% Pt/γ-Ga_2O_3 catalysts. OH concentration was calculated from CO-TPR based on (CO+OH→CO_2+1/2H_2) using n(OH)=2×n(H_2).

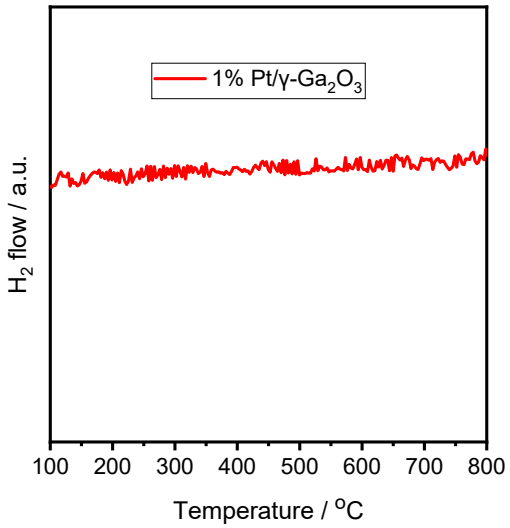

Figure S7 H_2 temperature-programmed reduction (H_2-TPR) test of 1% Pt/γ-Ga_2O_3.

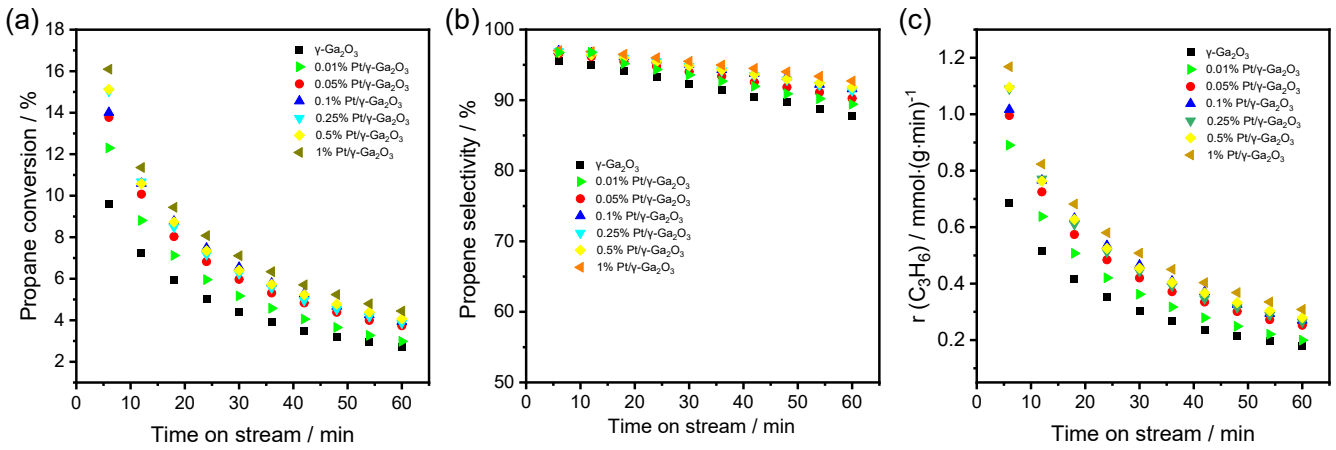

Figure S8 The dependence of (a) propane conversion, (b) propene selectivity, (c) rate of propene formation ($r(C_3H_6)$) and time on stream over x% Pt/γ-Ga_2O_3 catalysts in PDH reaction. Reaction temperature: 550°C, feed composition: 40% C_3H_8 in N_2.

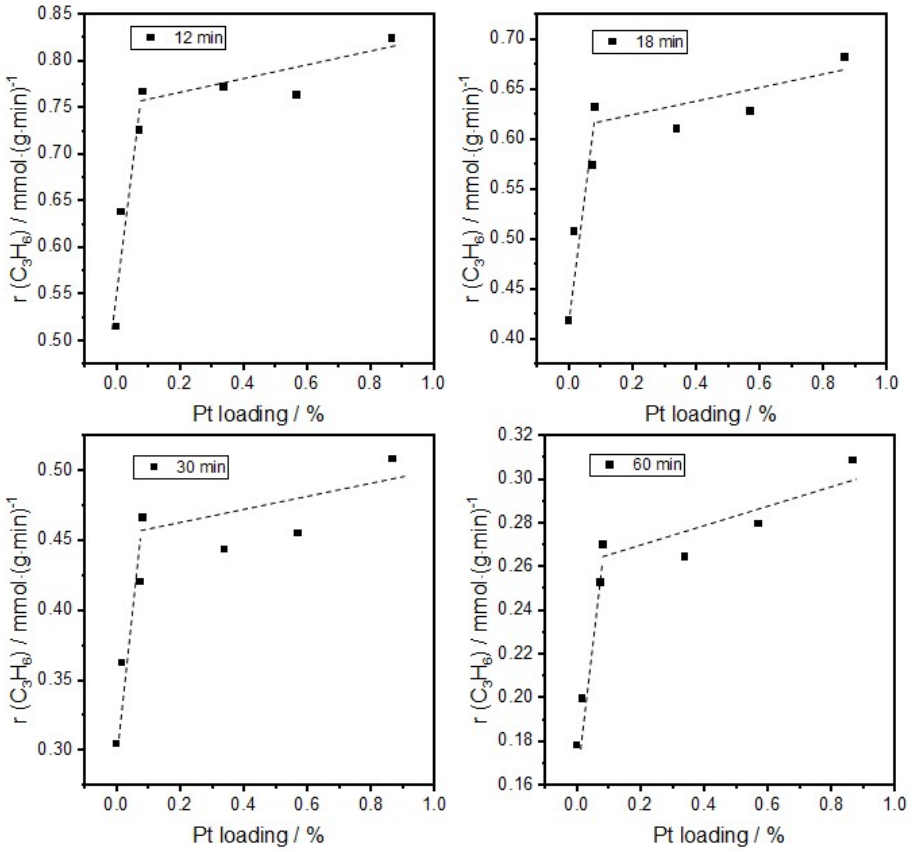

Figure S9 The relationship between the rate of propene formation ($r(C_3H_6)$) and Pt loading on different time on stream.

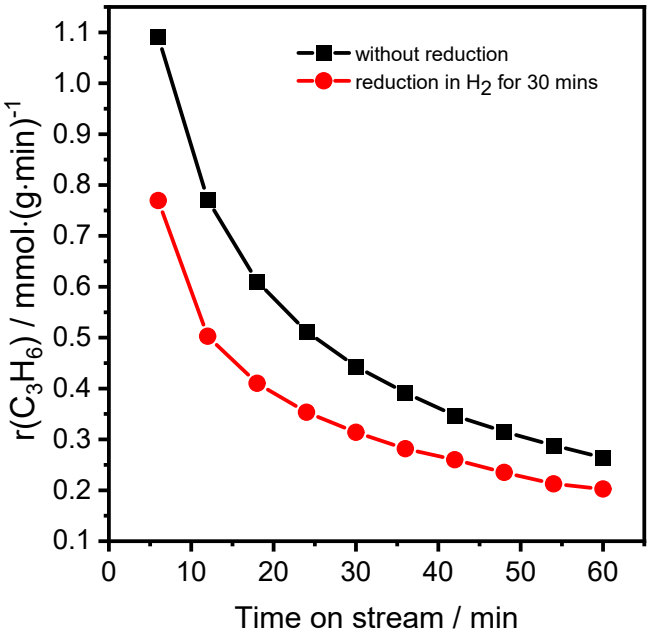

Figure S10 The relationship between the rate of propene formation and time on stream over 0.25% Pt/γ-Ga_2O_3 under different reduction treatments. Reaction temperature: 550 °C, feed composition: 40% C_3H_8 in N_2.

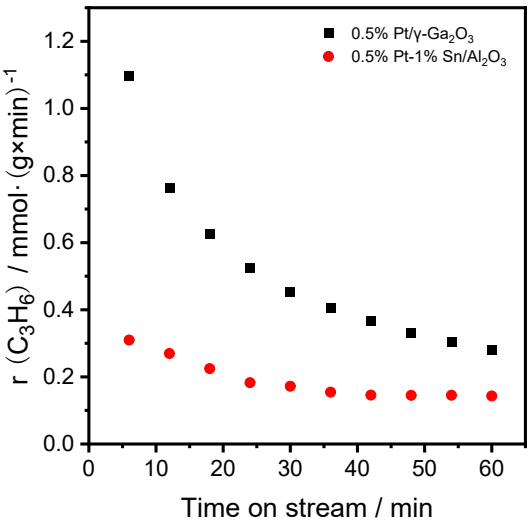

Figure S11 .Comparison of time-on-stream propene formation rates during propane dehydrogenation over 0.5 wt.% Pt/γ-Ga_2O_3 and 0.5 wt.% Pt–1 wt.% Sn/Al_2O_3. Reaction temperature: 550 °C, feed composition: 40% C_3H_8 in N_2.

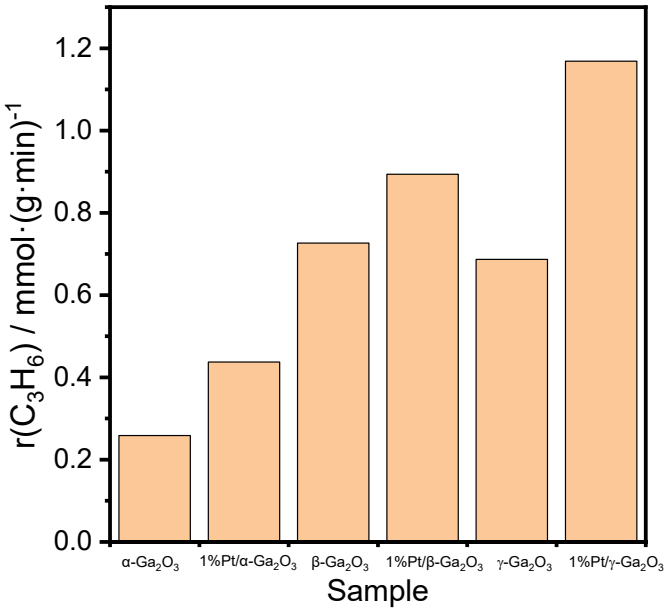

Figure S12 The rate of propene formation over α-Ga_2O_3, β-Ga_2O_3 and γ-Ga_2O_3 their corresponding Pt-supported catalysts.

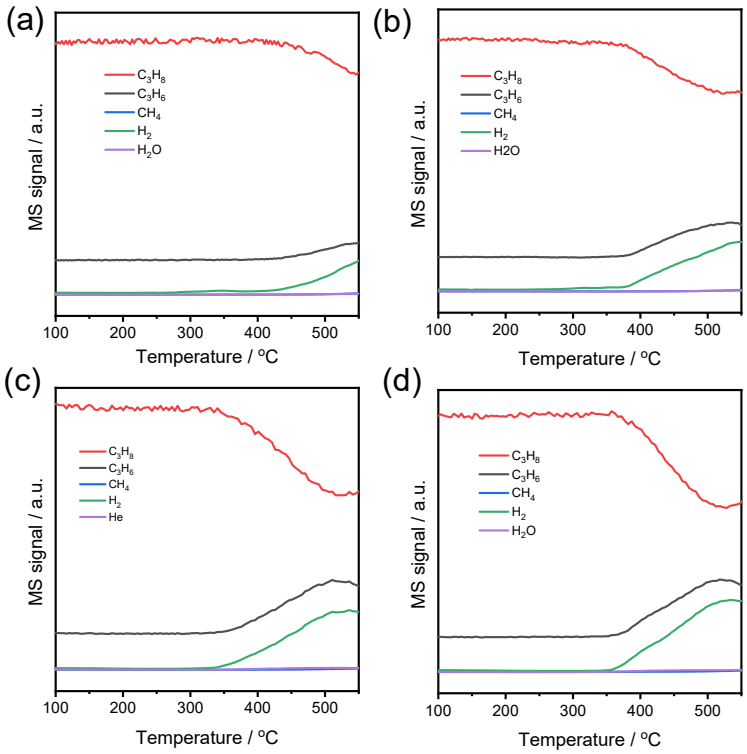

Figure S13 The MS signal intensity of C_3H_8, H_2, and H_2O recorded in propane temperature-programmed surface reaction (C_3H_8-TPSR) tests over (a) γ-Ga_2O_3, (b) 0.05%Pt/γ-Ga_2O_3, (c) 0.5%Pt/γ-Ga_2O_3, and (d) 1%Pt/γ-Ga_2O_3.

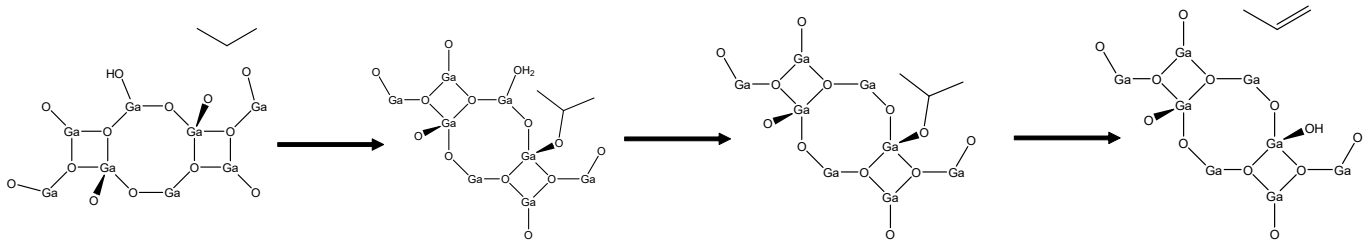

Figure S14 The closed PDH reaction cycle over γ-Ga_2O_3-OH surface.

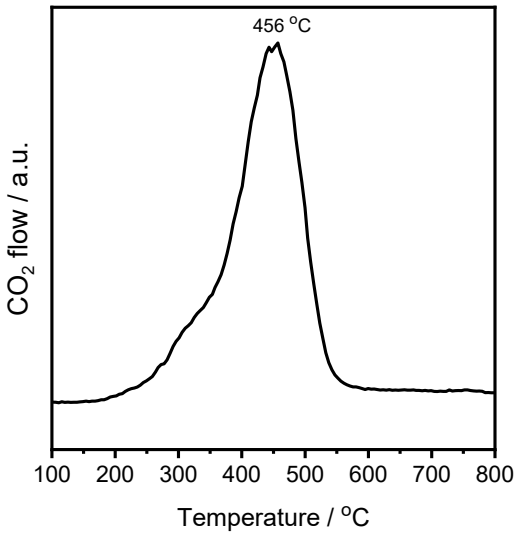

Figure S15 Temperature-programmed oxidation (TPO) tests of the spent 1% Pt/γ-Ga_2O_3 from activity test in PDH.

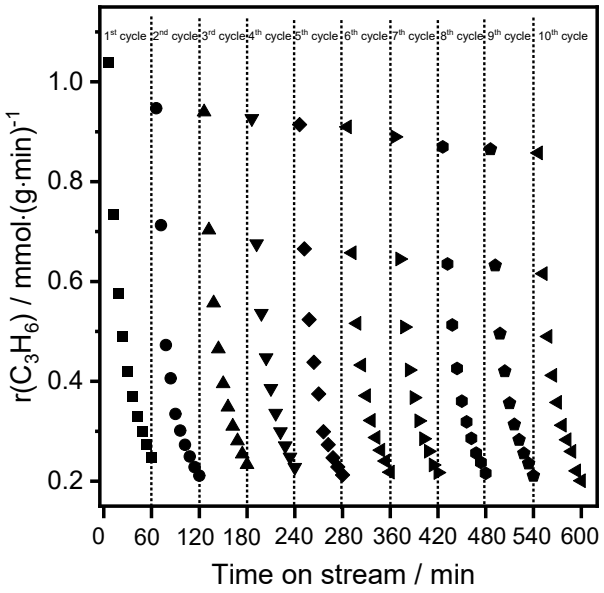

Figure S16 Reaction-regeneration stability of 1%Pt/γ-Ga_2O_3in the PDH reaction.

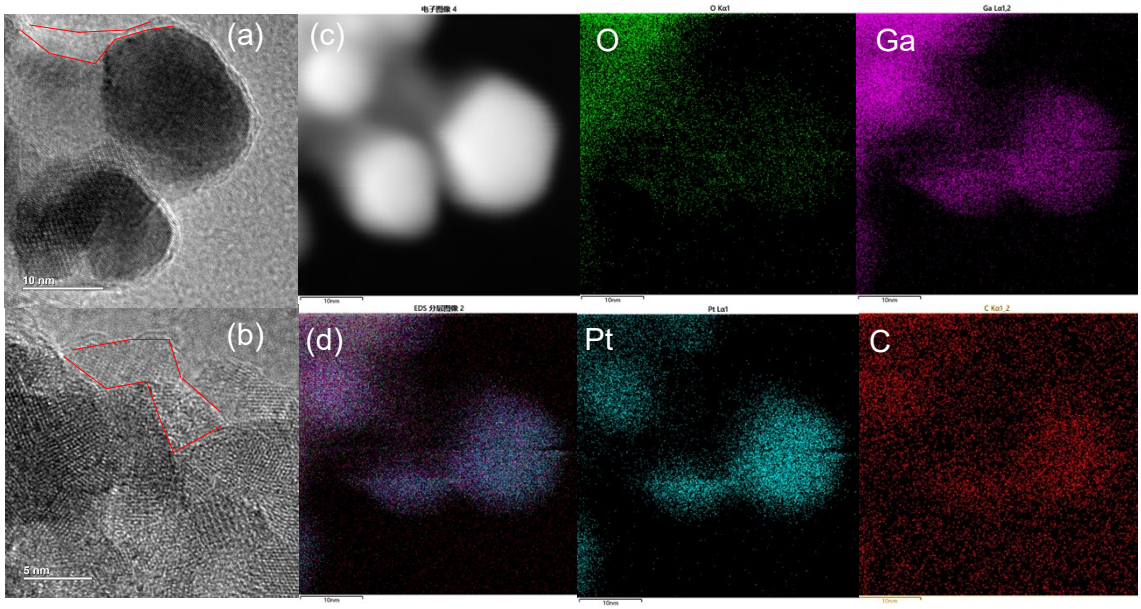

Figure S17 HRTEM images (a-b) of 1%Pt/γ-Ga_2O_3 to identify coke, and (c and d) EDS mapping of 1%Pt/γ-Ga_2O_3.

Table S1 The physiochemical properties including surface area, Pt content, and Pt dispersion degree, and the rate of propene formation, Y_{Pt} and TOF for different Pt/γ-Ga_2O_3 catalysts.

Catalysts	S_{BET} / $m^2 \cdot g^{-1}$	Pt content / wt.%	Dispersion degree / %	$r(C_3H_6)$ / $mmol \cdot g^{-1} \cdot min^{-1}$	Y_{Pt} / min^{-1}	TOF / min^{-1}
γ-Ga_2O_3	89	/	/	0.69	/	
0.01% Pt/γ-Ga_2O_3	78	0.016	/	0.89	10.85	
0.05% Pt/γ-Ga_2O_3	78	0.074	35.7	0.99	2.62	7.35
0.1% Pt/γ-Ga_2O_3	79	0.083	/	1.02	2.38	
0.25% Pt/γ-Ga_2O_3	82	0.340	/	1.09	0.62	
0.5% Pt/γ-Ga_2O_3	83	0.570	26.0	1.10	0.37	1.44
1% Pt/γ-Ga_2O_3	83	0.870	6.1	1.20	0.26	4.29

Estimated uncertainties: BET surface area ±1-2%; Pt content (ICP) ±1%; Pt dispersion (CO chemisorption) ±0.5-1%; propene formation rate ±1-3%; Y_{Pt} and TOF uncertainties follow from rate and dispersion uncertainties.

Table S2 The calculated acid density of different Pt/γ-Ga_2O_3 catalysts as obtained from NH_3-TPD tests. Estimated uncertainty: ±0.5-1%.

Catalysts	NH_3 desorbed (mmol·g^{-1})
γ-Ga_2O_3	0.089
0.01% Pt /γ-Ga_2O_3	0.075
0.05% Pt /γ-Ga_2O_3	0.083
0.1% Pt /γ-Ga_2O_3	0.075
0.25% Pt /γ-Ga_2O_3	0.056
0.5% Pt /γ-Ga_2O_3	0.062
1% Pt /γ-Ga_2O_3	0.062

Table S3 The calculated amount of CO consumption, CO_2 formation, H_2 formation and OH concentration over different Pt/γ-Ga_2O_3 catalysts in CO-TPR tests. Estimated uncertainty: ±0.2-0.5%.

Catalysts	CO consumption ($mmol \cdot g^{-1}$)	CO_2 ($mmol \cdot g^{-1}$)	H_2 ($mmol \cdot g^{-1}$)	OH concentration ($mmol \cdot g^{-1}$)
γ-Ga_2O_3	0.32	0.26	0.027	0.054
0.01%Pt/γ-Ga_2O_3	0.31	0.29	0.039	0.078
0.05% Pt /γ-Ga_2O_3	0.26	0.24	0.026	0.052
0.1% Pt /γ-Ga_2O_3	0.26	0.25	0.030	0.060
0.25% Pt /γ-Ga_2O_3	0.29	0.28	0.025	0.050
0.5% Pt /γ-Ga_2O_3	0.25	0.24	0.025	0.051
1% Pt /γ-Ga_2O_3	0.30	0.24	0.027	0.055

Note: OH concentration was calculated from CO-TPR based on $CO+OH \rightarrow CO_2+1/2H_2$ using $n(OH) = 2 \times n(H_2)$.

Table S4. The binding energies of $Ga2p_{3/2}$, $Pt4f_{5/2}$ and $Pt4f_{7/2}$, and the ratio of different Pt species (Pt^0, Pt^{2+}, and Pt^{4+}) over Pt/γ-Ga_2O_3 catalysts obtained from XPS results. Estimated uncertainty: ±0.1 eV.

Catalysts	Binding energy ($Ga2p_{3/2}$) / eV	Binding energy ($Pt4f_{5/2}$) / eV	Binding energy ($Pt4f_{7/2}$) / eV	Species	Ratio / %
γ-Ga_2O_3	1117.4				
0.05% Pt /γ-Ga_2O_3	1117.8	71.1	74.5	Pt^0	62.49
		72.6	75.9	Pt^{2+}	24.43
		73.8	77.2	Pt^{4+}	13.08
0.5% Pt /γ-Ga_2O_3	1118.0	70.1	73.4	Pt^0	31.61
		71.3	74.6	Pt^{2+}	45.51
		72.8	76.2	Pt^{4+}	22.88
1% Pt /γ-Ga_2O_3	1117.7	69.6	72.9	Pt^0	32.19
		70.6	73.9	Pt^{2+}	52.84
		72.3	75.6	Pt^{4+}	14.97

Note: XPS peak fitting were performed using MultiPak software with the Direct Fit routine. All spectra were calibrated to C 1s = 284.8 eV. A Shirley-type background was applied prior to curve fitting. Peaks were fitted using an asymmetric line-shape function. The Pt 4f region was analyzed using the double fitting option, which generates the Pt $4f_{7/2}$ and Pt $4f_{5/2}$ components simultaneously and applies physically meaningful constraints, including fixed spin–orbit splitting and fixed area ratio between the two components. Separate doublets corresponding to Pt^0, Pt^{2+}, and Pt^{4+} were included based on literature-reported binding energies and optimized to minimize residual error. The Ga 2p region was treated using the same fitting strategy. The fitted peak areas were used to calculate the $Pt^0/Pt^{2+}/Pt^{4+}$ ratios reported in Table S4. The uncertainty in fitted binding-energy positions is ±0.05–0.10 eV after charge correction (C 1s = 284.8 eV).

Table S5 The products selectivity including methane, ethane, ethene, and propene for all prepared Ga_2O_3 catalysts during the PDH reaction. Estimated uncertainty: ±0.5%.

Catalysts	S(CH_4) / %	S(C_2H_6) / %	S(C_2H_4) / %	S(C_3H_6) / %
γ-Ga_2O_3	1.62	0.29	2.5	95.59
0.01% Pt /γ-Ga_2O_3	0	1.60	1.70	96.70
0.05% Pt /γ-Ga_2O_3	1.26	0.38	1.79	96.57
0.1% Pt /γ-Ga_2O_3	1.08	0.33	1.61	96.98
0.25% Pt /γ-Ga_2O_3	1.12	0.43	1.57	96.88
0.5% Pt /γ-Ga_2O_3	1.10	0.44	1.66	96.80
1% Pt /γ-Ga_2O_3	1.05	0.47	1.48	97.01